Biosensors and Bioelectronics 33 (2012) 279–283

Contents lists available at SciVerse ScienceDirect

Biosensors and Bioelectronics

journal homepage: www.elsevier.com/locate/bios

Short communication

Electrochemical growth of gold nanoparticles on horizontally aligned carbon nanotubes: A new platform for ultrasensitive DNA sensing

Ling Li [a], Shun Wang [a,*], Ting Yang [a], Shaoming Huang [a], Jichang Wang [b,**]

[a] Nano-materials and Chemistry Key Laboratory, Wenzhou University, Wenzhou, Zhejiang, 325027, China
[b] Department of Chemistry and Biochemistry, University of Windsor, Windsor, ON, N9B 3P4, Canada

ARTICLE INFO

Article history:
Received 5 November 2011
Received in revised form
14 December 2011
Accepted 20 December 2011
Available online 27 December 2011

Keywords:
Au nanoparticles
DNA
Electrochemical impedance sensor
SWCNT array

ABSTRACT

A new platform based on electrochemical growth of Au nanoparticles on horizontally aligned single walled carbon nanotube (SWCNT) array was developed for ultrasensitive DNA detection. The as-prepared DNA-functionalized SWCNT-Au platform, in which every gold-coated SWCNT acts as an isolated micro electrode, could detect lower than 10 zmol complimentary 10-base DNA, which corresponded to having 6 DNA molecules in a 1 mL sample solution. For a 1-base mismatched DNA, the experimental detection limit was 100 amol. A linear relationship between the change of charge transfer resistance and target DNA concentration was achieved at low concentration range. Over the extended DNA concentration range, the change of charge transfer resistance was found to have a linear relationship with respect to the logarithm of the target DNA concentration. The sensor also showed great stability and could be conveniently regenerated via dehybridization in hot water. The significant improvement in sensitivity illustrates that combining Au nanoparticles with the on-site fabricated SWCNT array represents a promising platform for achieving ultrasensitive biosensor.

1. Introduction

Driving by the strong demand in gene analysis and forensic applications, various techniques based on optical (Agnes et al., 2010; Ferguson et al., 1996; Lassalle et al., 2001; Star et al., 2006), mechanical (Riahi et al., 2011; Munge et al., 2009), electrical and electrochemical (Zhong et al., 2009; Pei et al., 2010; De et al., 2008) processes have been developed for DNA and protein detection (Marti et al., 2007; Zhang et al., 2007). For the application of earlier diagnosis, where the analyte concentration is very low, developing a simple, rapid, low-cost and highly sensitive and selective assay platform remains a challenging and critical subject (Drummond et al., 2003; He and Dai, 2004; Chen et al., 2003; Zhang et al., 2009). A key issue with any DNA hybridization biosensor is how to enhance the probe DNA immobilization amount, and maintain the accessibility of probe DNA for hybridization detection. Recent advances in nano materials science offered unforeseeable opportunity of making new sensitive biosensors. Electrochemical sensor with nanostructured surface does not only offer significantly increased surface area for attaching probe molecules, but also exhibits improved electrochemical properties and beneficial orientation effects in probe immobilization (Pei et al., 2010; Chumbimuni-Torres et al., 2006).

Earlier studies have explored using carbon nanotubes (Tang et al., 2006; Kong et al., 2000; Collins et al., 2000; Weizmann et al., 2011) and/or gold nanoparticles (NPs) (Pinwattana et al., 2010; Lu et al., 2007; Spadavecchia et al., 2005; Kohli et al., 2004) to detect DNA and achieved favorable results. The Xu and Fang group showed, for example, that CdS nanoparticles could be utilized for signal amplification, which lowered the detection limit down to 1.43×10^{-10} M (Xu et al., 2004). Bonnani et al. utilized streptavidin-coated gold nanoparticles for improving the charge transfer resistance and reported the improvement of the detection limit from 26.5 pmol to 11.8 pmol in 140 μl solution (Bonanni et al., 2008). The Li and Zhang group utilized gold nanoparticles electrodeposited on the glassy carbon electrode for the immobilization of the thiolated aptamer, and achieved the lowest detection limit of 0.03 nM (Li et al., 2008).

Park and co-worker have recently reviewed progresses on electrochemical impedance spectroscopy (EIS) based DNA hybridization sensors (Park and Park, 2009). Previously we reported that using aligned single walled carbon nanotube (SWCNT) array could dramatically improved the sensitivity and selectivity of glucose detection (Jiang et al., 2011). This research was attempted to construct a new label-free platform for DNA biosensor through electrochemically growing Au NPs on the on-site fabricated horizontally aligned SWCNT array. Remarkably, the obtained DNA biosensor exhibited excellent response to target DNA.

* Corresponding author. Tel.: +86 577 86689357; fax: +86 577 88373111.
** Corresponding author.
E-mail addresses: shunwang@wzu.edu.cn (S. Wang), jwang@uwindsor.ca (J. Wang).

0956-5663/$ – see front matter © 2011 Elsevier B.V. All rights reserved.
doi:10.1016/j.bios.2011.12.039

2. Materials and method

2.1. Reagents

Analytical grade $HAuCl_4{\cdot}4H_2O$, $K_3[Fe(CN)_6]$ and tris-hydroxymethyl-aminomethane were purchased from Sigma. All oligonucleotide fragments were purchased from Shanghai Sangon Biological Engineering Technology & Services Co. Ltd. (China). EIS was performed with an Autolab PGSTAT30 electrochemical analysis system supplied with a FRA 2.0 module (Netherland). EIS experiments were performed at room temperature with a conventional three-electrode system comprising a platinum foil auxiliary electrode, saturated Ag/AgCl reference electrode, and SWCNT-Au or DNA modified SWCNT-Au working electrode. The electrolyte contained 5.0 mM $K_3[Fe(CN)_6]$ and 0.10 M KCl. The frequency range was from 100 mHz to 10 kHz at a potential of 0.17 V and a voltage amplitude of 5 mV. Deionized water was prepared with a Milli-Q system (18.2 MΩ cm, Millipore, and USA). All probes were HPLC purified and their base sequences were: probe DNA 5′-SH-$(CH_2)_6$-CCCCATCCCC-3′, target DNA 5′-GGGGATGGGG-3′, 1-base mismatched DNA 5′-GGGGTTGGGG-3′, 3-base mismatched DNA 5′-GGGGCCCGGG-3′.

2.2. Fabrication of SWCNT-Au electrode

All SWCNT arrays were prepared on SiO_2/Si wafer according to our previous work (Huang et al., 2008). The electrochemical growth of Au NPs was performed by using the horizontally oriented SWCNT array as the working electrode and Pt wire as an auxiliary electrode. Au NPs were electrochemically deposited on the working electrode at a constant potential of −0.5 V for 10 s in a deoxygenated 1.0 mM $HAuCl_4$ solution.

The freshly obtained SWCNT-Au electrode was incubated at 4 °C in a 50 mM Tris–HCl buffer solution (pH 8.0) containing 1.0 μM probe DNA for 10 h. During this process the single-stranded DNA (ssDNA) self-assembled on the SWCNT-Au electrode. Afterwards, the SWCNT-Au-ssDNA electrode was carefully washed with Milli-Q water to remove any trace of unassembled probe ssDNA. The thus-obtained electrode is denoted as SWCNT-Au-ssDNA in this study. DNA hybridization of the SWCNT-Au-ssDNA electrode was carried out by immersing it in a target DNA solution of various concentrations at 42 °C for 2 h. After that, the hybridized electrode was thoroughly rinsed with a 0.2% sodium dodecylsulfate phosphate buffer (pH 7.3) to remove nonhybridized target DNA and then washed with Milli-Q water to remove phosphate buffer. Scheme 1 illustrates how the DNA-functionalized SWCNT-Au platform was constructed in this research.

3. Results and discussion

The scanning electron microscopy (SEM) image in Fig. 1a illustrates that the SWCNT array consists of nanotubes that are over 250 m in length. Since most of the SWCNT are parallel with each other, each SWCNT shall act as an isolated electrode. The visible increase in the diameter and the surface roughness of these SWCNTs in Fig. 1b indicates the deposition of Au NPs. SEM image in Fig. 1c indicates that those Au NPs have dendritic microstructure and bound tightly to those SWCNT. The energy dispersive X-ray (EDX) spectrum in Fig. 1d further confirms the successful growth of Au NPs. Careful examination of the SEM images indicates that Au NPs have been successfully produced on every SWCNT. The surface area of the SWCNT-Au platform was estimated with Randkes-Sevcik equation ($i_p = 0.4463nFAC(nF\nu D/RT)^{1/2}$) (see Supplementary document Fig. S1).

The sensitivity of SWCNT-Au-ssDNA electrode was examined in Fig. 2A, where EIS of $Fe(CN)_6^{3-}$/$Fe(CN)_6^{4-}$ redox reaction was measured after the probe electrode was first hybridized in solutions containing different amounts of complimentary target DNA. Semicircles in the Nyquist plots implicate that the reduction of $Fe(CN)_6^{3-}$ is an electron-transfer limited process. It is interesting to point out that there are two semicircles in the EIS obtained here. The first one has the same magnitude diameter as that observed in a vertical SWCNT array (Siddiqui et al., 2010), implying that the first semicircle in Fig. 2A is likely due to the resistance of SWCNT array. The second semicircle in EIS arises from the resistance to charge transfer from the redox probe $Fe(CN)_6^{3-}$/$Fe(CN)_6^{4-}$ to the Au NPs electrode surface. This resistance, R_{ct}, varies with the property of the DNA film and can thus be employed to determine DNA concentration in a sample. Upon the immobilization of probe ssDNA there is indeed a significant increase in R_{ct} (see curve b). It is because the self-assembled monolayer of ssDNA hinders electron transfer of $Fe(CN)_6^{3-}$/$Fe(CN)_6^{4-}$ at the electrode surface due to electrostatic interactions etc.

When the SWCNT-Au-ssDNA electrode was employed to measure complimentary DNA solution, increasing R_{ct} was obtained with respect to the increase of target DNA concentration (see EIS curves c to f in Fig. 2A). It is because hybridization of probe ssDNA with target DNA results in the formation of increasing amounts of double-stranded DNA (ds-DNA). ds-DNA subsequently enhances the electrostatic interaction between the redox marker

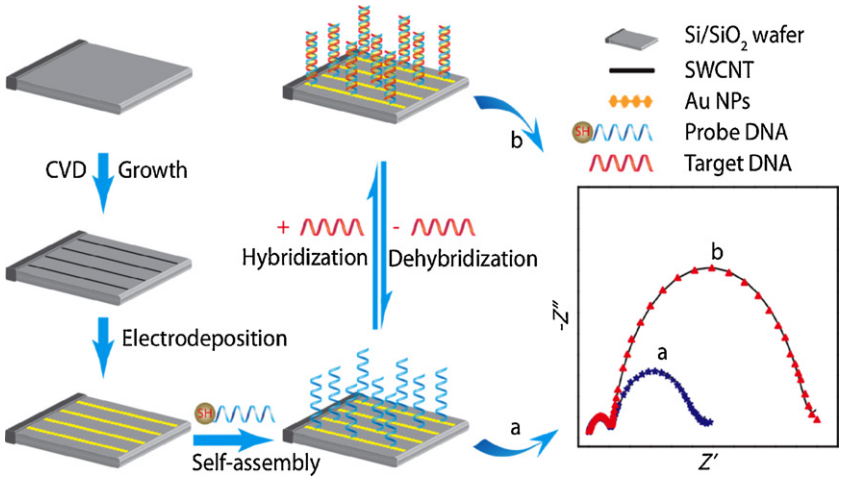

Scheme 1. Illustration of the experimental procedure.

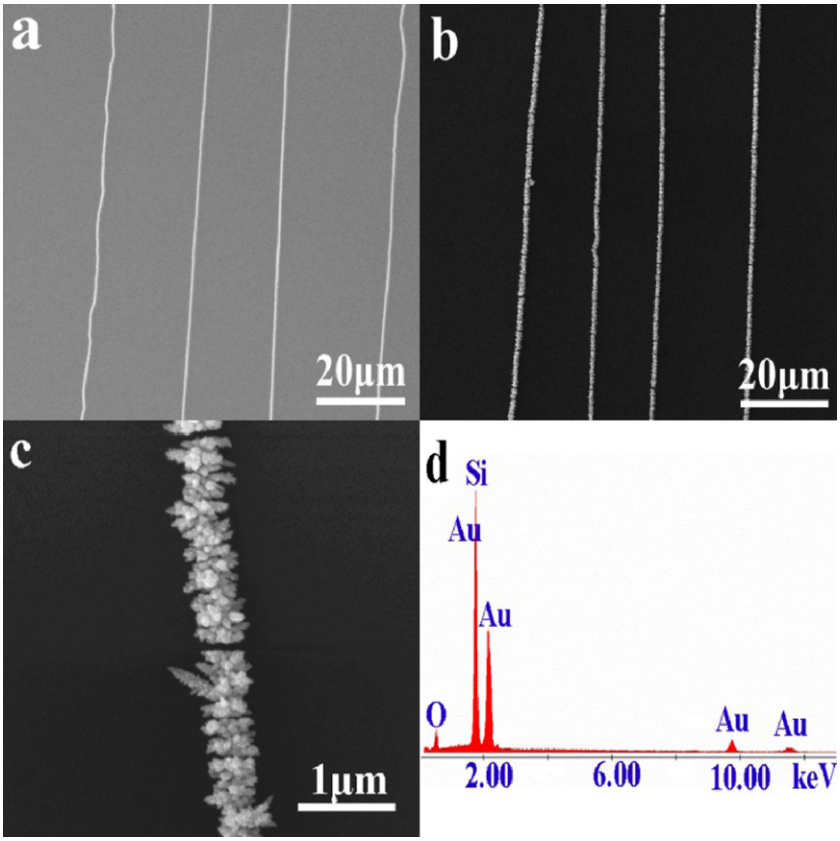

Fig. 1. SEM images of (a) SWCNT array, (b) SWCNT-Au array, (c) single SWCNT-Au electrode and (d) EDX spectrum of SWCNT-Au array.

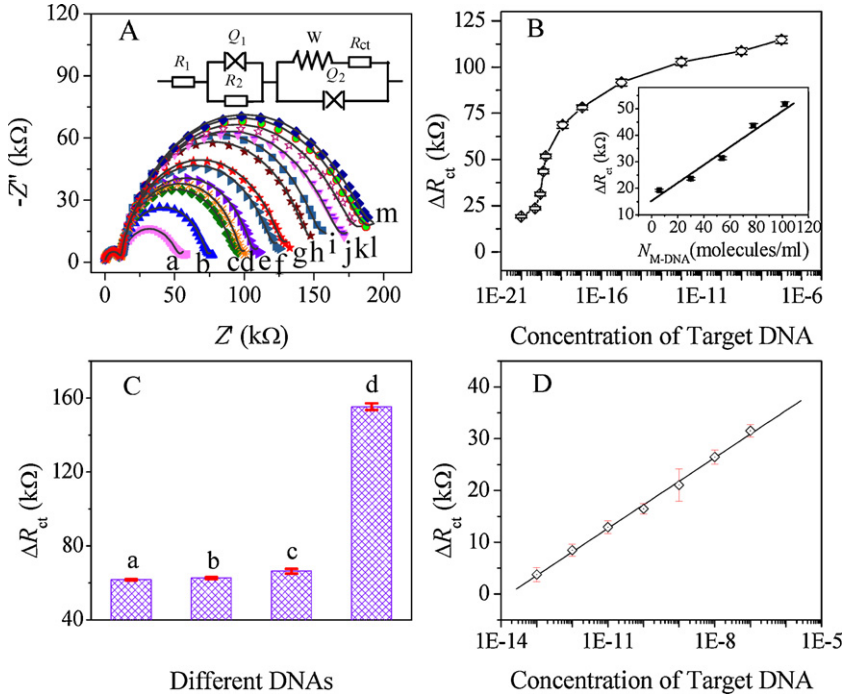

Fig. 2. (A) Nyquist plots ($-Z''$ vs Z') for (a) SWCNT-Au and (b to m) SWCNT-Au-ssDNA electrodes hybridized with the following amounts of complimentary DNA: (b) 0, (c) 1.0×10^{-20} M, (d) 5.0×10^{-20} M, (e) 9.0×10^{-20} M, (f) 1.3×10^{-19} M, (g) 1.7×10^{-19} M, (h) 1.2×10^{-18} M, (i) 1.1×10^{-17} M, (j) 1.0×10^{-15} M, (k) 1.0×10^{-12} M, (l) 1.0×10^{-9} M, and (m) 1.0×10^{-7} M. The inset shows the equivalent circuit of the EIS responses. (B) Plot of ΔR_{ct} vs the concentration of target DNA. The inset shows a linear relationship between ΔR_{ct} and the number of target DNA molecules. (C) ΔR_{ct} measured at SWCNT-Au-ssDNA electrodes hybridized with (a) 0 M, (b) 0.1 pM 3-base mismatched, (c) 0.1 pM 1-base mismatched, and (d) 0.1 pM complimentary target DNAs; (D) ΔR_{ct} as a function of 1-base mismatched target DNA concentration.

and the backbone of the oligonucleotide and may as well introduce intercalation effect between the redox marker and ds-DNA. As a result, the charge transfer of $Fe(CN)_6^{3-}/Fe(CN)_6^{4-}$ redox reaction was further hindered. Note that from measurements c to f, the SWCNT-Au-ssDNA electrode was not dehybridized after each measurement, instead additional amount of target DNA was added to the hybridized solution. The corresponding increase in the charge transfer resistance R_{ct} indicates that at low target DNA concentrations only part of the probe ssDNA was hybridized.

The EIS measurements illustrate that a detectable increase in the charge transfer resistance could be attained for the target DNA concentration as low as 1.0×10^{-21} M, which corresponds to having 6 DNA molecules in a 1.0 ml analyte sample. In other words, the actual lowest experimentally detected concentration (LOEDC) is 10 zmol. This result highlights the feasibility of using a microelectrode sensor to detect single DNA molecule. To test whether this newly fabricated platform works for long oligonucleotide sequences, the number of DNA bases was increased to 21. The preliminary data indicates that the LOEDC could also reach 1.0×10^{-18} M. More systematic investigation of long oligonucleotide sequences will be reported later.

All the above experimental impedance spectra have been fitted to an equivalent circuit model (see the inset in Fig. 2A). R_1 denotes the solution resistance, i.e. a resistance between the reference and SWCNT-Au-ssDNA working electrode. In the absence of a constant temperature, there was a small fluctuation in R_1, ranging from 0.1 to 0.4 kΩ. The combination of R_2 and Q_1 accounts for the behavior of SWCNT array and Au NPs film. A notable difference between the EIS achieved here and those obtained with other DNA hybridization sensors is that here there are two semicircles. Based on the similarity with the size of the semicircle reported in vertically aligned SWCNT array (Siddiqui et al., 2010), here the first semicircle (i.e. R_2) is suggested to arise from SWCNT array and Q_1 accounts for the capacitance between SWCNT and gold film. The constant phase element Q_2 accounts for the capacitance of DNA film on the electrode. It acts as a nonlinear capacitor accounting for the inhomogeneity of the DNA films. A Warburg impedance (W) was seen with the SWCNT-Au bare electrode or SWCNT-Au-ssDNA electrode at low target DNA concentrations. The fitting also suggests that a Warburg impedance is needed to achieve a good agreement between simulated and experimental EIS. Fig. 2B indicates that electrodes prepared in this study are effective over a broad concentration range. A linear relationship between ΔR_{ct} and target DNA concentration was achieved at low concentrations (see the inset in Fig. 2B). The regression equation was found to be $\Delta R_{ct} = 0.34 N_{M\text{-}DNA} + 15.3$ with $R = 0.98$ ($N_{M\text{-}DNA}$ denotes the number of complimentary DNA molecules/ml). Over the extended DNA concentration range, ΔR_{ct} was found to have a linear relationship with respect to the logarithm of target DNA concentration, where the regression equation is $\Delta R_{ct} = 3.67\log[\text{M-DNA}] + 142.3$ with a correlation coefficient of 0.985.

The selectivity of this SWCNT-Au-ssDNA electrode was examined in Fig. 2 C, where responses to a 1-base mismatched, 3-base mismatched and complimentary DNAs were depicted. A single-nucleotide mismatch introduced disorder into the ds-DNA film, weakening the interaction between the redox probe and ds-DNA. It consequently allowed the redox probe to penetrate into the film to a larger extent. As a result, the R_{ct} value was reduced. For 3-base mismatched target DNAs, more disorders were introduced into the ds-DNA film, and the R_{ct} became nearly the same as that of SWCNT-Au-ssDNA bare electrode. The great R_{ct} difference between complimentary and 1-base mismatched target DNA illustrates that the functionalized SWCNT-Au platform is highly selective. The selectivity remains even at the target DNA concentration as low as 0.1 pM, which corresponds to 100 amol DNA in a 1.0 ml sample solution. Fig. 2D shows that there is a linear relationship between ΔR_{ct} and the logarithm of one-base mismatched target DNA concentration over the range from 0.1 pM to 100 nM with a function of $\Delta R_{ct} = 4.58\log[\text{target-DNA}] + 63.04$ ($R = 0.998$) (target-DNA denotes 1-base mismatched DNA).

The reusability of the above SWCNT-Au-ssDNA electrode was analyzed via measuring against 1.0×10^{-20} M complimentary DNAs. After each measurement, the electrode was regenerated upon dehybridization in hot water (Li et al., 2007). After each cycle, R_{ct} of the SWCNT-Au-ssDNA electrode was found to increase slightly. The obtained R_{ct} of 1.0×10^{-20} M complimentary DNA also increases slightly after every dehybridization (<1%). When ΔR_{ct} was calculated, the variation became even smaller (Supplementary document Fig. S2). The SWCNT-Au-ssDNA electrode used to measure non-complimentary DNA is easier to regenerate than that used to measure complimentary target DNA. Such a difference has been attributed to the nonspecific adsorption and the incompact interaction between the mismatched DNA strands (Li et al., 2007).

4. Conclusion

This study prepared a new platform for DNA detection, which is based on electrochemical growth of Au NPs on horizontally aligned SWCNT array. Combining with the simple and convenient EIS technique, the as-prepared sensor exhibited ultrahigh sensitivity, great selectivity and reusability, in which the 10-base DNA detection limit was experimentally found to be as low as 10 zmol. The ultrahigh sensitivity makes it an attractive selection for earlier diagnosis of various diseases. The significant improvement of this platform over those utilizing SWCNT or Au NPs alone indicates synergistic interactions of horizontal SWCNT array and Au NPs. When those horizontally aligned SWCNT were replaced by random SWCNT matrix, changes in the R_{ct} decreases, unveiling the unique advantages of horizontally aligned SWCNT array electrodes as a new platform in biosensing.

Acknowledgments

We are grateful for financial supports from NSFC (51025207, 21073133 and 20843007), Zhejiang Provincial Natural Science Foundation of China (Y4080177, Y4090248 and Y5100283) and Zhejiang scientific and technological innovation fund (2010R424047, 2011R424045).

Appendix A. Supplementary data

Supplementary data associated with this article can be found, in the online version, at doi:10.1016/j.bios.2011.12.039.

References

Agnes, R.S., Jernigan, F., Shell, J.R., Sharma, V., Lawrence, D.S., 2010. J. Am. Chem. Soc. 132, 6075–6080.
Bonanni, A., Esplandiu, M.J., del Valle, M., 2008. Electrochim. Acta 53, 4022–4029.
Chen, R.J., Bangsaruntip, S., Drouvalakis, K.A., Wong, S.K., Shim, M., Li, Y., Kim, W., Utz, P.J., Dai, H., 2003. Proc. Natl. Acad. Sci. U.S.A. 100, 4984–4989.
Chumbimuni-Torres, K.Y., Dai, Z., Rubinova, N., Xiang, Y., Pretsch, E., Wang, J., Bakker, E., 2006. J. Am. Chem. Soc. 128, 13676–13677.
Collins, P.G., Bradley, K., Ishigami, M., Zettl, A., 2000. Science 287, 1801–1804.
De, M., Ghosh, P.S., Rotello, V.M., 2008. Adv. Mater. 20, 4225–4241.
Drummond, T.G., Hill, M.G., Barton, J.K., 2003. Nat. Biotechnol. 21, 1192–1199.
Ferguson, J.A., Boles, T., Adams, C., Walt, D., Nat, D., 1996. Biotechnology 14, 1681–1684.
He, P.G., Dai, L.M., 2004. Chem. Commun. 3, 348–349.
Huang, S.M., Qian, Y., Chen, J.Y., Cai, Q.R., Wan, L., Wang, S., Hu, W.B., 2008. J. Am. Chem. Soc. 130, 11860–11861.
Jiang, F., Wang, S., Lin, J.J., Jin, H.L., Zhang, L.J., Huang, S.M., Wang, J.C., 2011. Electrochem. Commun. 13, 363–365.
Kohli, P., Harrell, C.C., Cao, Z.H., Gasparac, R., Tan, W.H., Martin, C.R., 2004. Science 305, 984–986.

Kong, J., Franklin, N.R., Zhou, C., Chapline, M., Peng, S., Cho, K., Dai, H., 2000. Science 287, 622–625.
Lassalle, N., Vieil, E., Correia, J.P., Abrantes, L.M., 2001. Biosens. Bioelectron. 16, 295–303.
Li, D.L., Zou, X.Q., Shen, Q., Dong, S.J., 2007. Electrochem. Commun. 9, 191–196.
Li, X.X., Shen, L.H., Zhang, D.D., Qi, H.L., Gao, Q., Ma, F., Zhang, C.X., 2008. Biosens. Bioelectron. 23, 1624–1630.
Lu, W.S., Lin, L., Jiang, L., 2007. Biosens. Bioelectron. 22, 1101–1105.
Marti, A.A., Jockusch, S., Stevens, N., Ju, J.Y., Turro, N.J., 2007. Acc. Chem. Res. 40, 402–409.
Munge, B.S., Krause, C.E., Malhotra, R., Patel, V., Dutkind, J.S., Rusling, J.M., 2009. Electrochem. Commun. 11, 1009–1012.
Park, J.Y., Park, S.M., 2009. Sensors 9, 9513–9532.
Pei, H., Lu, N., Wen, Y., Song, S., Liu, Y., Yan Fan, H.C., 2010. Adv. Mater. 22, 4754–4758.
Pinwattana, K., Wang, J., Lin, C.T., Wu, H., Du, D., Lin, Y.H., Chailapakul, O., 2010. Biosens. Bioelectron. 26, 1109–1113.
Riahi, R., Mach, K.E., Mohan, R., Liao, J.C., Wong, P.K., 2011. Anal. Chem. 83, 6349–6354.
Siddiqui, S., Arumugam, P.U., Chen, H., Li, J., Meyyappan, M., 2010. ACS Nano 4, 955–961.
Spadavecchia, J., Prete, P., Lovergine, N., Tapfer, L., Rella, R., 2005. J. Phys. Chem. B 109, 17347–17349.
Star, A., Tu, E., Niemann, J., Gabriel, J.C.P., Joiner, C.S., Valcke, C., 2006. Proc. Natl. Acad. Sci. U.S.A. 103, 921–926.
Tang, X., Bansaruntip, S., Nakayama, N., Yenilmez, E., Chang, Y., Wang, Q., 2006. Nano Lett. 6, 1632–1636.
Weizmann, Y., Chenoweth, D.M., Swager, T.M., 2011. J. Am. Chem. Soc. 133, 3238–3241.
Xu, Y., Cai, H., He, P.G., Fang, Y.Z., 2004. Electroanalysis 16, 150–155.
Zhang, J., Song, S.P., Wang, L.H., Pan, D., Fan, C.H., 2007. Nat. Protoc. 2, 2888–2895.
Zhang, X.Z., Jiao, K., Liu, S.F., Hu, Y.W., 2009. Anal. Chem. 81, 6006–6012.
Zhong, H., Lei, X., Hun, X., Zhang, S., 2009. Chem. Commun. 45, 6958–6960.